Relativistic mean-field approximation in a density dependent parametrization model at finite temperature

S. S. Avancini,[1] M. E. Bracco,[2] M. Chiapparini,[2] and D. P. Menezes[1]
[1]*Departmento de Física, CFM—Universidade Federal de Santa Catarina, Florianópolis, Santa Catarina, Caixa Postal 476, CEP 88.040-900, Brazil*
[2]*Instituto de Fıisica, Universidade do Estado do Rio de Janeiro, Rua São, Francisco Xavier 524, Maracanã CEP 20559-900, Rio de Janeiro, RJ, Brazil*

(Received 18 November 2002; published 4 February 2003)

In this work we calculate the relativistic equation of state of nuclear matter for different proton fractions at zero and finite temperatures within the Thomas-Fermi approach considering three different parameter sets: the well-known NL3 and TM1 and a density-dependent parametrization proposed by Typel and Wolter. The main differences are outlined, and the consequences of imposing β stability in these models are discussed.

DOI: 10.1103/PhysRevC.67.024301 PACS number(s): 21.65.+f, 21.30.−x, 25.70.−z

I. INTRODUCTION AND FORMALISM

Understanding the properties of nuclear matter at both normal and high densities is of crucial importance in explaining the appearance of neutron stars after the supernova explosion and the formation of transiron elements in nuclear reactions.

One of the most popular relativistic models is the nonlinear Walecka model [1,2], which can be used in order to obtain different equations of state (EOS) as far as different parameter sets are employed. This model was extended in several ways to include many-body correlations as density-dependent meson couplings in the relativistic Lagrangian [3–6]. In this work we investigate the consequences in the EOS when the parametrizations of the well-known NL3 model [7], which is a good parametrization in describing finite nuclei properties, are changed to the density-dependent one proposed in Ref. [8]. The new parametrization is determined by fitting several nuclear matter bulk properties and also some finite nuclei. Both models were investigated considering two types of proton fractions: fixed ones and those arising when β equilibrium is incorporated. Some considerations are also done in relation with the TM1 parameter set [9]. The extension of the density-dependent parametrization to finite temperature EOS is also investigated. This extension has been partially studied in Ref. [10] for symmetric nuclear matter only. In nuclear collisions involving stable or radioactive neutron rich nuclei, in experiments yielding nuclear multifragmentation, in protoneutron stars, among innumerous examples, the resulting matter is known to carry a reasonable amount of isospin asymmetry. Hence, in the present work, a more complete and detailed study is performed in order to account for asymmetric matter as well.

We start from the Lagrangian density of the relativistic nonlinear model, adapted in order to accommodate the NL3, TM1 forces and the density-dependent meson-nucleon coupling constants [8]:

$$\begin{aligned}\mathcal{L}=&\bar{\psi}\left[\gamma_\mu\left(i\partial^\mu-\Gamma_\omega\omega^\mu-\frac{\Gamma_\rho}{2}\vec{\tau}\cdot\vec{\rho}^\mu\right)-(M-\Gamma_\sigma\sigma)\right]\psi\\&+\frac{1}{2}(\partial_\mu\sigma\partial^\mu\sigma-m_\sigma^2\sigma^2)-\frac{1}{3!}\kappa\sigma^3-\frac{1}{4!}\lambda\sigma^4-\frac{1}{4}\omega_{\mu\nu}\omega^{\mu\nu}\\&+\frac{1}{2}m_\omega^2\omega_\mu\omega^\mu+\frac{1}{4!}\xi\Gamma_\omega^4(\omega_\mu\omega^\mu)^2-\frac{1}{4}\vec{\rho}_{\mu\nu}\cdot\vec{\rho}^{\mu\nu}\\&+\frac{1}{2}m_\rho^2\vec{\rho}_\mu\cdot\vec{\rho}^\mu,\end{aligned}\tag{1}$$

where σ, ω^μ, and $\vec{\rho}^{\vec{\mu}}$ are the scalar-isoscalar, vector-isoscalar, and vector-isovector meson fields respectively, $\omega_{\mu\nu}=\partial_\mu\omega_\nu-\partial_\nu\omega_\mu$, and $\vec{\rho}_{\mu\nu}=\partial_\mu\vec{\rho}_\nu-\partial_\nu\vec{\rho}_\mu-\Gamma_\rho(\vec{\rho}_\mu\times\vec{\rho}_\nu)$. Besides this, M is the nucleon mass, m_σ, m_ω, m_ρ are the masses of the mesons and Γ_σ, Γ_ω, Γ_ρ are the nucleon-meson coupling constants. κ, λ, and ξ are the self-interacting scalar and vector coupling constants. In this work we investigate the differences arising from three parameter sets, namely, NL3 [7], TM1 [9], and TW [8]. In the first two cases, Γ_σ, Γ_ω, and Γ_ρ are the usual g_σ, g_ω, and g_ρ. In the second case, the density-dependent coupling constants are adjusted in order to reproduce some of the nuclear matter bulk properties, using the following parametrization:

$$\Gamma_i(\rho)=\Gamma_i(\rho_{sat})f_i(x),\quad i=\sigma,\omega\tag{2}$$

with

$$f_i(x)=a_i\frac{1+b_i(x+d_i)^2}{1+c_i(x+d_i)^2},\tag{3}$$

where $x=\rho/\rho_{sat}$ and

$$\Gamma_\rho(\rho)=\Gamma_\rho(\rho_{sat})\exp[-a_\rho(x-1)],\tag{4}$$

with the values of the parameters m_j, Γ_j, a_j, b_i, c_i, and d_i, $j=\sigma,\omega,\rho$ given in Ref. [8]. Other possibilities for these

TABLE I. Nuclear matter properties.

	NL3 [7]	TM1 [9]	TW [8]
B/A(MeV)	16.3	16.3	16.3
ρ_0 (fm^{-3})	0.148	0.145	0.148
K(MeV)	272	281	240
$\mathcal{E}_{sym.}$ (MeV)	37.4	36.9	32.0
M^*/M	0.60	0.63	0.56

parameters are also found in the literature [10]. In the TW parametrization the meson self-coupling constants κ, λ, and ξ are zero. The nuclear matter bulk properties described by these three parameter sets are displayed in Table I.

From the Euler-Lagrange equations we obtain the field equations of motion in the mean-field approximation for infinite matter, where the meson fields are replaced by their expectation values. In this approximation, the expectation value of the σ, ω, and ρ meson fields are called ϕ_0, V_0, and b_0, respectively. The coupled equations read

$$m_\sigma^2\phi_0+\frac{1}{2}\kappa\phi_0^2+\frac{1}{3!}\lambda\phi_0^3-\Gamma_\sigma\rho_s=0, \tag{5}$$

$$m_\omega^2 V_0+\frac{1}{3!}\xi\Gamma_\omega^4 V_0^3-\Gamma_\omega\rho=0, \tag{6}$$

$$m_\rho^2 b_0-\frac{\Gamma_\rho}{2}\rho_3=0, \tag{7}$$

$$\left[i\gamma^\mu\partial_\mu-\gamma_0\left(\Gamma_\omega V_0+\frac{\Gamma_\rho}{2}\tau_3 b_0+\Sigma_0^R\right)-M^*\right]\psi=0, \tag{8}$$

where the *rearrangement* term Σ_0^R is given by

$$\Sigma_0^R=\frac{\partial\Gamma_\omega}{\partial\rho}\rho V_0+\frac{\partial\Gamma_\rho}{\partial\rho}\rho_3\frac{b_0}{2}-\frac{\partial\Gamma_\sigma}{\partial\rho}\rho_s\phi_0, \tag{9}$$

and the scalar and baryonic densities are defined as

$$\rho_s=\langle\bar{\psi}\psi\rangle, \tag{10}$$

$$\rho=\langle\bar{\psi}\gamma^0\psi\rangle, \tag{11}$$

$$\rho_3=\langle\bar{\psi}\gamma^0\tau_3\psi\rangle. \tag{12}$$

In the following discussion we consider nuclear matter in the the mean-field approximation only for the TW parameter set. Due to translational and rotational invariance the Lagrangian density reduces to

$$\mathcal{L}_{MFT}=\bar{\psi}\left[i\gamma_\mu\partial^\mu-\gamma_0\Gamma_\omega V_0-\gamma_0\frac{\Gamma_\rho}{2}\tau_3 b_0-(M-\Gamma_\sigma\phi_0)\right]\psi$$
$$-\frac{1}{2}m_\sigma^2\phi_0^2+\frac{1}{2}m_\omega^2 V_0^2+\frac{1}{2}m_\rho^2 b_0^2. \tag{13}$$

The conserved energy-momentum tensor can be derived in the usual fashion [11],

$$\mathcal{T}^{\mu\nu}_{MFT}=\bar{\psi}i\gamma^\mu\partial^\nu\psi-g^{\mu\nu}\left[\frac{1}{2}m_\sigma^2\phi_0^2-\frac{1}{2}m_\omega^2 V_0^2-\frac{1}{2}m_\rho^2 b_0^2\right.$$
$$\left.-\bar{\psi}\gamma_0\Sigma_0^R\psi\right]. \tag{14}$$

Note that the rearrangement term included above and defined in Eq. (9) assures the energy-momentum conservation, i.e., $\partial_\mu\mathcal{T}^{\mu\nu}=0$. From the energy-momentum tensor one easily obtains the Hamiltonian operator

$$\mathcal{H}_{MFT}=\int d^3x\,\mathcal{T}^{00}_{MFT}=\int d^3x\;\psi^\dagger\left(-i\vec{\alpha}\cdot\boldsymbol{\nabla}+\beta M^*+\Gamma_\omega V_0\right.$$
$$\left.+\frac{\Gamma_\rho}{2}\tau_3 b_0\right)\psi+V(\tfrac{1}{2}m_\sigma^2\phi_0^2-\tfrac{1}{2}m_\omega^2 V_0^2-\tfrac{1}{2}m_\rho^2 b_0^2), \tag{15}$$

where $M^*=M-\Gamma_\sigma\phi$ and V is the volume of the system. In the above equation the rearrangement term cancels out. Notice that as a consequence, the energy density does not carry the rearrangement term either and can be written in the semiclassical Thomas-Fermi approximation as

$$\mathcal{E}=2\sum_{i=p,n}\int\frac{d^3p}{(2\pi)^3}\sqrt{\mathbf{p}^2+M^{*2}}(f_{i+}+f_{i-})+\Gamma_\omega V_0\rho$$
$$+\frac{\Gamma_\rho}{2}b_0\rho_3+\frac{m_\sigma^2}{2}\phi_0^2-\frac{m_\omega^2}{2}V_0^2-\frac{m_\rho^2}{2}b_0^2. \tag{16}$$

Note that for the NL3 parametrization, the term $\kappa\phi_0^3/6+\lambda\phi_0^4/24$ also appears in the energy density equation and for the TM1 these two terms come together with $-\xi\Gamma_\omega^4 V_0^4/24$. Following the notation in Ref. [12], the thermodynamic potential can be written as

$$\Omega=\mathcal{E}-T\mathcal{S}-\mu_p\rho_p-\mu_n\rho_n, \tag{17}$$

where $\mathcal{S}$ is the entropy density of a classical Fermi gas, T is the temperature, μ_p (μ_n) is the proton (neutron) chemical potential, and ρ_p and ρ_n are, respectively, the proton and neutron densities calculated in such a way that $\rho=\rho_p+\rho_n$. We have

$$\rho_i=2\int\frac{d^3p}{(2\pi)^3}(f_{i+}-f_{i-}),\quad i=p,n, \tag{18}$$

where the distribution functions f_{i+} and f_{i-} for particles and antiparticles have to be derived in order to make the thermo-

dynamic potential stationary for a system in equilibrium. After straightforward substitutions, Eq. (17) becomes

$$\Omega = 2\sum_{i=p,n}\int \frac{d^3p}{(2\pi)^3}\sqrt{\mathbf{p}^2+M^{*2}}(f_{i+}+f_{i-}) + \Gamma_\omega V_0\rho + \frac{\Gamma_\rho}{2}b_0\rho_3 + \frac{m_\sigma^2}{2}\phi_0^2 - \frac{m_\omega^2}{2}V_0^2 - \frac{m_\rho^2}{2}b_0^2 + 2T\sum_{i=p,n}\int \frac{d^3p}{(2\pi)^3}\left[f_{i+}\ln\left(\frac{f_{i+}}{1-f_{i+}}\right)+\ln(1-f_{i+}) + f_{i-}\ln\left(\frac{f_{i-}}{1-f_{i-}}\right)+\ln(1-f_{i-})\right] - 2\sum_{i=p,n}\int\frac{d^3p}{(2\pi)^3}\mu_i(f_{i+}-f_{i-}). \quad (19)$$

For a complete demonstration of the above shown expressions obtained in a Thomas-Fermi approximation for the nonlinear Walecka model, please refer to Ref. [12]. At this point, Eq. (19) is minimized in terms of the distribution functions for fixed meson fields, i.e.,

$$\left.\frac{\partial\Omega}{\partial f_{i+}}\right|_{f_{i-},f_{j\pm},\phi_0,V_0,b_0} = 0 \quad i\neq j. \quad (20)$$

For the proton distribution function, the above calculation yields

$$E^*(\mathbf{p}) + \Sigma_0^R - \mu_p + \Gamma_\omega V_0 + \frac{\Gamma_\rho}{2}b_0 = -T\ln\left(\frac{f_{p+}}{1-f_{p+}}\right), \quad (21)$$

where $E^*(\mathbf{p})=\sqrt{\mathbf{p}^2+M^{*2}}$. Similar equations, with some sign differences are obtained for the antiproton, neutron, and antineutron distribution functions. The effective chemical potentials are then defined as

$$\mu_p^* = \mu_p - \Gamma_\omega V_0 - \frac{\Gamma_\rho}{2}b_0 - \Sigma_0^R,$$

$$\mu_n^* = \mu_n - \Gamma_\omega V_0 + \frac{\Gamma_\rho}{2}b_0 - \Sigma_0^R, \quad (22)$$

and the following equations for the distribution functions can be written as

$$f_{i\pm} = \frac{1}{1+\exp[(E^*(\mathbf{p})\mp\mu_i^*)/T]}, \quad i=p,n. \quad (23)$$

In the above calculation we have used

$$\rho_s = 2\sum_{i=p,n}\int\frac{d^3p}{(2\pi)^3}\frac{M^*}{E^*(\mathbf{p})}(f_{i+}+f_{i-})$$

and $\rho_3=\rho_p-\rho_n$. The proton fraction is defined as $Y_p=\rho_p/\rho$.

Within the Thomas-Fermi approach the pressure becomes

$$P = \frac{1}{3\pi^2}\sum_{i=p,n}\int dp\frac{\mathbf{p}^4}{\sqrt{\mathbf{p}^2+M^{*2}}}(f_{i+}+f_{i-}) - \frac{m_\sigma^2}{2}\phi_0^2\left(1+2\frac{\rho}{\Gamma_\sigma}\frac{\partial\Gamma_s}{\partial\rho}\right) + \frac{m_\omega^2}{2}V_0^2\left(1+2\frac{\rho}{\Gamma_\omega}\frac{\partial\Gamma_\omega}{\partial\rho}\right) + \frac{m_\rho^2}{2}b_0^2\left(1+2\frac{\rho}{\Gamma_\rho}\frac{\partial\Gamma_\rho}{\partial\rho}\right). \quad (24)$$

In the NL3 model, the term $-\kappa\phi_0^3/6-\lambda\phi_0^4/24$ is also present in Eq. (24), and in the TM1 model these terms are also accompanied by $\xi\Gamma_\omega^4V_0^4/24$. It is also important to stress that the thermodynamical consistency which requires the equality of the pressure calculated from the thermodynamical definition and from the energy-momentum tensor, discussed in Ref. [14], is also obeyed by the temperature-dependent TW model.

Another quantity of interest is the nuclear bulk symmetry energy discussed in Ref. [15]. It is usually defined as

$$\mathcal{E}_{sym} = \frac{1}{2}\left.\frac{\partial^2\mathcal{E}}{\partial\delta^2}\right|_{\delta=0}, \quad (25)$$

with $\delta=\rho_3/\rho$ and which can be analytically rewritten as

$$\mathcal{E}_{sym} = \left(\frac{k_F^2}{6E^*(\mathbf{p})}+\frac{\Gamma_\rho^2}{8m_\rho^2}\right)\rho, \quad (26)$$

where

$$k_{Fp}=k_F(1+\delta)^{1/3}, \quad k_{Fn}=k_F(1-\delta)^{1/3},$$

with $k_F=(1.5\pi^2\rho)^{1/3}$. The value and behavior of the symmetry energy at densities larger than nuclear saturation density are still not well established. This quantity is important in studies involving neutron stars and radioactive nuclei. In general, relativistic and nonrelativistic models give different predictions for the symmetry energy. A comparison between the symmetry energies coming from the NL3 and TW models is also discussed in the present work.

II. CONSIDERING β STABILITY

At this point, we introduce the ideas of β stability and charge neutrality. In an ideal system of protons, neutrons, electrons, and muons in equilibrium, the particle levels are filled in such a way that the β decays are forbidden. In order to study the conditions of β equilibrium, one has to incorporate leptonic degrees of freedom in the Lagrangian density of equation (1). As far as the leptons exchange mesons neither with the baryons nor with themselves, they can be introduced as free Fermi gases, as usually done in the literature. The weak interaction beteween leptons and hadrons is taken into account through the constraint of charge neutrality. The new Lagrangian density reads

$$\mathcal{L}_{lb} = \mathcal{L} + \mathcal{L}_{leptons}, \quad (27)$$

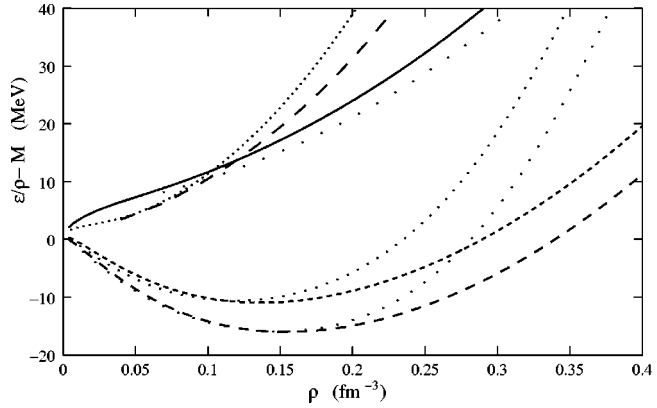

FIG. 1. Binding energy in terms of the baryon density for different proton fractions and $T=0$. From top to bottom we show the EOS with β stability for NL3 (dotted line) and for TW (long-dashed line); $Y_p=0$ for NL3 (solid line) and TW (large spaced dotted line); $Y_p=0.3$ for NL3 and TW and $Y_p=0.5$ for NL3 and TW.

where

$$\mathcal{L}_{leptons}=\sum_l \bar{\psi}_l(i\gamma_\mu\partial^\mu-m_l)\psi_l, \tag{28}$$

$\mathcal{L}$ is given in Eq. (1) and l describes the two lightest leptons, i.e., the electron and the muon, whose masses are, respectively, $m_e=0.511$ MeV and $m_\mu=106.55$ MeV. The expressions for the energy density $\mathcal{E}_{lb}$ and the pressure P_{lb} are also modified by the leptons, reading

$$\mathcal{E}_{lb}=\mathcal{E}+2\sum_l \int \frac{d^3p}{(2\pi)^3}\sqrt{\mathbf{p}^2+m_l^2}(f_{l+}+f_{l-}) \tag{29}$$

with

$$f_{l\pm}=\frac{1}{1+\exp[(\epsilon\mp\mu_l)/T]}, \quad l=e,\mu, \tag{30}$$

where μ_l being the chemical potentials for leptons of type l, $\epsilon=\sqrt{\mathbf{p}^2+m_l^2}$ and

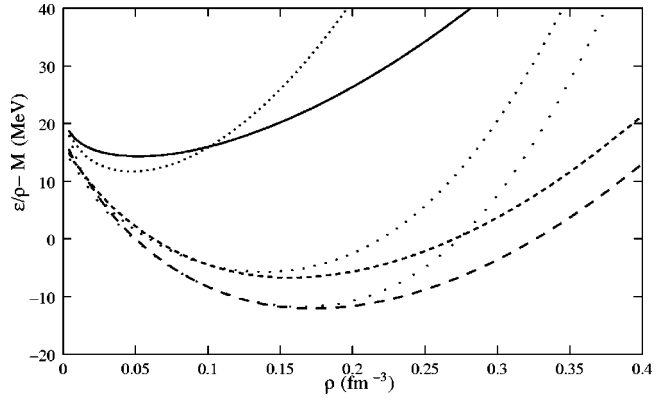

FIG. 2. Binding energy in terms of the baryon density for different proton fractions and $T=10$ MeV. From top to bottom we show the EOS with $Y_p=0$ for NL3 and TW; $Y_p=0.3$ for NL3 and TW; $Y_p=0.5$ for NL3 and TW.

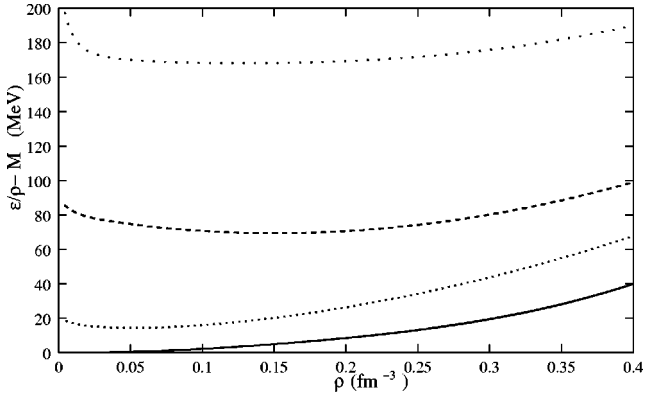

FIG. 3. Binding energy in terms of the baryon density for different temperatures, $Y_p=0$ and TW. From top to bottom we show the EOS for $T=100$ MeV, $T=50$ MeV, $T=10$ MeV, and $T=0$.

$$P_{lb}=P+\frac{1}{3\pi^2}\sum_l \int \frac{\mathbf{p}^4 dp}{\sqrt{\mathbf{p}^2+m_l^2}}(f_{l+}+f_{l-}), \tag{31}$$

where $\mathcal{E}$ and P are given by Eqs. (16) and (24), respectively.

Notice that the leptons are considered as a gas of noninteracting relativistic particles, in such a way that the minimization of the thermodynamic potential is not altered by their presence. The already mentioned requirement of charge neutrality yields

$$\rho_p=\rho_e+\rho_\mu, \tag{32}$$

where the electron and muon densities can be read off from Eq. (18) by substituting i by l. From the condition of chemical equilibrium in the weak processes, obtained from the minimization of the Gibbs potential with the conditions of baryon number and electric charge conservation, one is left with the following relations between the chemical potentials:

$$\mu_p=\mu_n-\mu_e, \tag{33}$$

$$\mu_\mu=\mu_e. \tag{34}$$

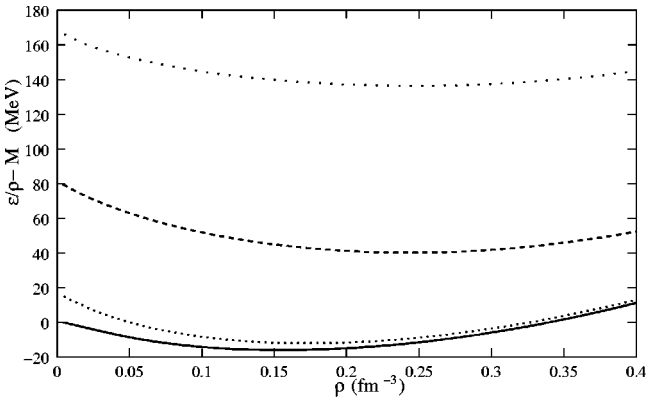

FIG. 4. Binding energy in terms of the baryon density for different temperatures, $Y_p=0.5$ and TW. From top to bottom we show the EOS for $T=100$ MeV, $T=50$ MeV, $T=10$ MeV, and $T=0$.

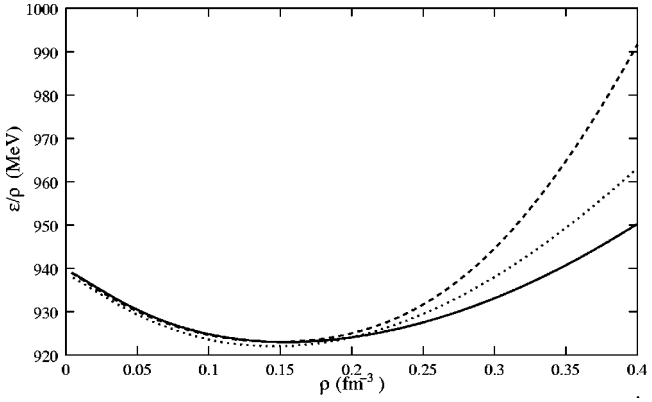

FIG. 5. Energy density per nucleon in terms of the baryon density for zero temperature and $Y_p=0.5$. From top to bottom we show the EOS for NL3, TM1, and TW.

Common definitions for the lepton fractions are $Y_l=\rho_l/\rho$, although the lepton densities are not part of the baryon density. Some consequences of the imposition of β stability in relativistic models are discussed in Ref. [16].

III. RESULTS AND CONCLUSIONS

In this work, as in other recent papers (Ref. [9], for instance), the important range of temperature which should be discussed lies between 10 and 150 MeV since the liquid-gas phase transition takes place around 10 MeV and the phase transition from hadronic to quarkionic matter around 150 MeV.

In Fig. 1 we show the zero temperature EOS for different proton fractions and two of the parameter sets used in this work, i.e., NL3 and TW. The TW parametrization makes the EOS softer not only for symmetric nuclear matter ($Y_p=0.5$), as discussed in Ref. [8], but also for all other proton fraction possibilities. The same is true if β stability is imposed. In Fig. 2 the EOS is plotted for $T=10$ MeV and again, a behavior similar to that of Fig. 1 is observed. Notice, however, that the minima of all curves are shifted upwards and that the curves for $Y_p=0$, which do not exhibit minima for $T=0$ acquire them once the temperature increases.

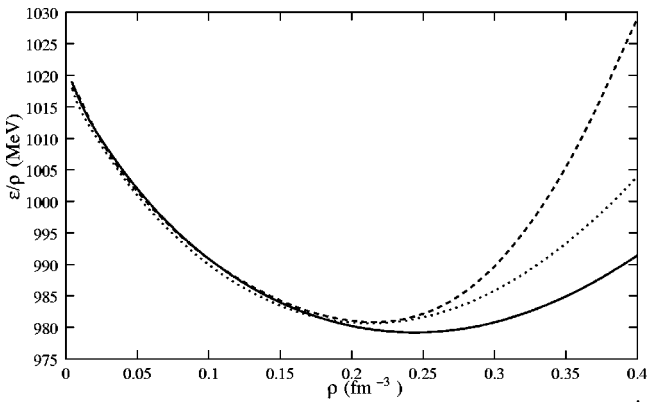

FIG. 6. Energy density per nucleon in terms of the baryon density for $T=50$ MeV and $Y_p=0.5$. From top to bottom we show the EOS for NL3, TM1, and TW.

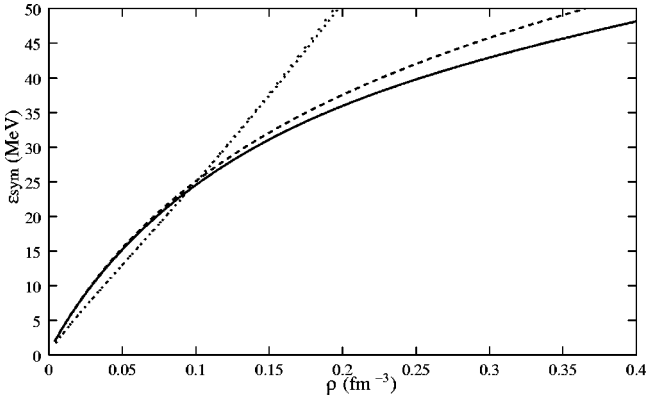

FIG. 7. Symmetry energy in terms of the baryon density, respectively, for $Y_p=0.0$ and 0.5 for NL3 (dotted curves) and TW (dashed and solid curves).

In Fig. 3 we show the EOS for neutron matter ($Y_p=0$) at different temperatures, namely, $T=0$, $T=10$ MeV, $T=50$ MeV, and $T=100$ MeV. At very low densities the inclination of the curves vary substancially from low to high temperatures. This is because in this region of low densities, the thermal energy kT is an appreciable fraction of the Fermy energy ϵ_F, making the effects of the temperature, in particular, the particle-antiparticle creation, more dramatic in this regime than at high densities, were ϵ_F is greater. In Fig. 4 the EOS is plotted, this time for symmetric nuclear matter. One can see the change in the minimum from a negative to a positive value, which becomes very large for high temperatures. One can also notice that the minima of all curves are slightly shifted to higer densities.

From the analysis of Figs. 1 and 2 we conclude that the TW parametrization is softer than the NL3 one. This can be explained looking for the Γ parametrizations (2) and (4) in the limit of $\rho/\rho_{sat}\gg 1$. In this limit we have

$$\Gamma_i(\rho)\to 0.7\Gamma_i(\rho_{sat}),\quad i=\sigma,\omega, \tag{35}$$

$$\Gamma_\rho(\rho)\to 0. \tag{36}$$

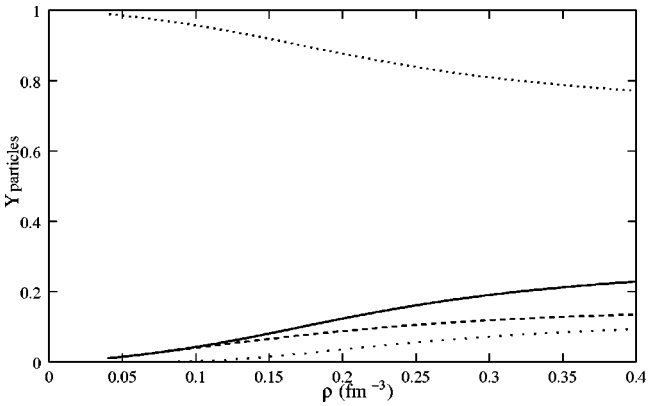

FIG. 8. Particle composition in terms of the baryon density for $T=0$ and NL3. From top to bottom we show the distribution of neutrons, protons, electrons, and muons.

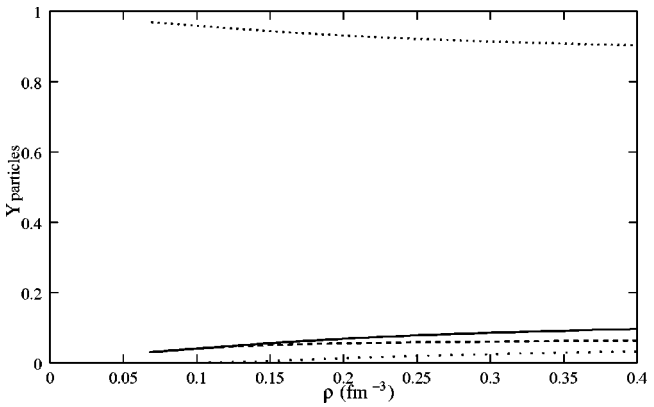

FIG. 9. Particle composition in terms of the baryon density for $T=0$ and TW. From top to bottom we show the distribution of neutrons, protons, electrons, and muons.

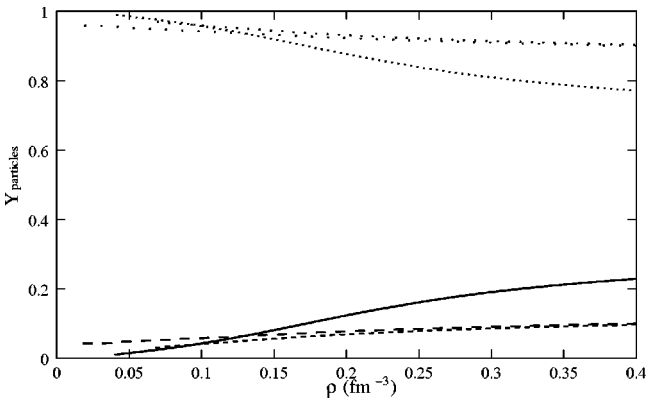

FIG. 10. Proton and neutron composition in terms of the baryon density. The upper curves shown the neutron composition and the lower ones show the proton composition. The curves which are practically coincident stand for the TW at $T=0$ and $T=10$ MeV. The other curves stand for the NL3 force.

At such high densities, the system interacts mainly through the exchange of the meson ω, once the scalar meson σ saturates as $m^*\rightarrow 0$. The Γ_ω coupling constant of the NL3 model is the same as at the saturation density, while Eq. (35) says that, in this limit, the Γ_ω coupling constant for the TW parametrization is lower than the value at the saturation point. TW is thus less repulsive at high densities than NL3, which makes its EOS softer. This fact has important consequences, for example, when modeling neutron stars. A soft EOS provides a neutron star with a total mass lower than the value obtained with a stiff EOS [13].

We have also checked that the TW parametrization provides an EOS softer than that obtained with the TM1 force [9] and closer to the relativistic Brueckner-Hartree-Fock (RBHF) EOS [17], as can be seen in Figs. 5 and 6 for $T=0$ and $T=50$ MeV and symmetric nuclear matter. Notice that the EOS which is stiffest at zero temperature remains so at higher temperatures. The same is true for other proton fractions. The RBHF theory produces well the nuclear matter saturation based on the nucleon-nucleon interaction determined by scattering experiments. The TM1 parametrization includes a nonlinear ω term, and hence works with one extra parameter which is also adjusted in order to reproduce nuclear matter bulk properties. We then conclude that the TW parameter set is a very useful force in the studies involving EOS at high densities.

In Fig. 7 the symmetry energy is displayed for NL3 and TW for pure neutron matter and symmetric nuclear matter. Different proton fractions give rise to slightly different curves because of the difference in Fermi momenta and in the effective mass, which enters in $E^*(\mathbf{p})$. According to Ref. [15], the symmetry energy at normal nuclear matter density is found to lay in between 27–36 MeV in the mass formula calculations, in the range of 28 to 38 MeV in nonrelativistic models and in between 35 and 42 MeV in relativistic models. Notice that at the saturation point, the value for the TW parametrization (32 MeV) is somewhat lower than for the NL3, remains in the accepted range of validity, and is closer to the predictions of nonrelativistic models. Moreover, the curves obtained for the TW model present a much smaller symmetry energy at larger densities and also a smoother behavior as compared with the curves arising from the NL3 model, which gives a more linear tendency to the curve. This result can be explained looking at Eq. (36), which tell us that Γ_ρ goes to zero at high densities, consequently so does its contribution in Eq. (26). On the opposite, Γ_ρ in the NL3 parametrization is constant as a function of density.

We have finally studied the particle composition once β stability is imposed. In Figs. 8 and 9 the particle composition obtained at $T=0$, respectively, for NL3 and TW are shown. In Fig. 10 we show the proton and neutron composition for NL3 and TW at $T=0$ MeV and TW at $T=10$ MeV. One can see that if the temperature does not increase much, the particle composition for a fixed parameter set remains basically the same. Nevertheless, it changes substancially from NL3 to TW. In particular, at high densities, we can see that TW is less isospin symmetric than NL3. This is due, again, to result (36), which says that, for TW, the ρ-nucleon interaction is suppressed at high densities. It is precisely this interaction which drives the systems to a more isospin symmetric configuration at high densities, as we can see in Fig. (8) for NL3, where this interaction survives in this limit.

An extension of this work in order to study liquid-gas phase transition and consequent droplet formation is currently under investigation.

ACKNOWLEDGMENTS

This work was partially supported by CNPq—Brazil. One of the authors (D.P.M.) would like to thank Dr. Constança Providência for very useful suggestions and productive discussions related to this work.

[1] J. Boguta and A.R. Bodmer, Nucl. Phys. **A292**, 413 (1977); A.R. Bodmer and C.E. Price, *ibid.* **A505**, 123 (1989); A.R. Bodmer, *ibid.* **A526**, 703 (1991).
[2] Y.K. Gambir, P. Ring, and A. Thimet, Ann. Phys. (N.Y.) **198**, 132 (1990); H. Berghammer, D. Vretenar, and P. Ring, Phys. Lett. B **296**, 290 (1992); D. Vretenar, H. Berghammer, and P. Ring, *ibid.* **319**, 29 (1993); H. Berghammer, D. Vretenar, and P. Ring, Nucl. Phys. **A560**, 1014 (1993).
[3] R.J. Furnstahl, B.D. Serot, and Tang Hua-Bin, Nucl. Phys. **A615**, 441 (1997).
[4] M. Chiapparini, A. Delfino, M. Malheiro, L.V. Belvedere, and A.O. Gattone, Z. Phys. A: Hadrons Nucl. **355**, 145 (1996).
[5] M. Chiapparini, A. Delfino, M. Malheiro, and A.O. Gattone, Z. Phys. A: Hadrons Nucl. **357**, 47 (1997).
[6] A. Delfino, F.S. Navarra, M. Nielsen, R.B. Prandini, and M. Chiapparini, Mod. Phys. Lett. A **14**, 1615 (1999).
[7] G.A. Lalazissis, J. König, and P. Ring, Phys. Rev. C **55**, 540 (1997).
[8] S. Typel and H.H. Wolter, Nucl. Phys. **A656**, 331 (1999).
[9] K. Sumiyoshi, H. Kuwabara, and H. Toki, Nucl. Phys. **A581**, 725 (1995).
[10] G. Hua, L. Bo, and M. Di Toro, Phys. Rev. C **62**, 035203 (2000).
[11] B. Serot and J. D. Walecka, *Advances in Nuclear Physics* (Plenum, New York, 1986), Vol. 16.
[12] D.P. Menezes and C. Providência, Phys. Rev. C **60**, 024313 (1999).
[13] N. K. Glendenning, *Compact Stars* (Springer-Verlag, Berlin, 1997).
[14] C. Fuchs, H. Lenske, and H.H. Wolter, Phys. Rev. C **52**, 3043 (1995).
[15] B.-A. Li, C.M. Ko, and W. Bauer, Int. J. Mod. Phys. E **7**, 147 (1997).
[16] A.L. Espıindola and D.P. Menezes, Phys. Rev. C **65**, 045803 (2002).
[17] R. Brockmann and R. Machleidt, Phys. Rev. C **42**, 1965 (1990).